Retinal abnormalities associated with the G90D mutation in opsin

ARTICLE *in* THE JOURNAL OF COMPARATIVE NEUROLOGY · OCTOBER 2004

Impact Factor: 3.23 · DOI: 10.1002/cne.20283 · Source: PubMed

THE JOURNAL OF COMPARATIVE NEUROLOGY 478:149–163 (2004)

Retinal Abnormalities Associated with the G90D Mutation in Opsin

MUNA I. NAASH,[1]* TING-HUAI WU,[2] DIBYENDU CHAKRABORTY,[1] STEVEN J. FLIESLER,[3] XI-QIN DING,[1] MAY NOUR,[1] NEAL S. PEACHEY,[4,5] JANIS LEM,[6] NASSER QTAISHAT,[2] MUAYYAD R. AL-UBAIDI,[1] AND HARRIS RIPPS[2]

[1]Department of Cell Biology, University of Oklahoma Health Sciences Center, Oklahoma City, Oklahoma 73104

[2]Department Ophthalmology and Visual Sciences, University of Illinois College of Medicine, Chicago, Illinois 60612

[3]Department Ophthalmology, Pharmacological and Physiological Science, St. Louis University School of Medicine, St. Louis, Missouri 63104-1540

[4]Research Service, Cleveland Veterans Affairs Medical Center, Cleveland, Ohio 44106

[5]Cole Eye Institute, Cleveland Clinic Foundation, Cleveland, Ohio 44195

[6]Department Ophthalmology and Molecular Cardiology, Tufts Center for Vision Research, Tufts-New England Medical Center, Boston, Massachusetts 02111-1533

ABSTRACT

Several mutations in the opsin gene have been associated with congenital stationary night blindness, considered to be a relatively nonprogressive disorder. In the present study, we examined the structural and functional changes induced by one of these mutations, i.e., substitution of aspartic acid for glycine at position 90 (G90D). Transgenic mice were created in which the ratio of transgenic opsin transcript to endogenous was 0.5:1, 1.7:1, or 2.5:1 and were studied via light and electron microscopy, immunocytochemistry, electroretinography (ERG), and spectrophotometry. Retinas with transgenic opsin levels equivalent to one endogenous allele ($G_{0.5}$) appeared normal for a period of about 3–4 months, but at later ages there were disorganized, shortened rod outer segments (ROS), and a loss of photoreceptor nuclei. Higher levels of G90D opsin expression produced earlier signs of retinal degeneration and more severe disruption of photoreceptor morphology. Despite these adverse effects, the mutation had a positive effect on the retinas of rhodopsin knockout ($R^{-/-}$) mice, whose visual cells fail to form ROS and rapidly degenerate. Incorporation of the transgene in the null background ($G^{+/-}/R^{-/-}$ or $G^{+/+}/R^{-/-}$) led to the development of ROS containing G90D opsin and prolonged survival of photoreceptors. Absorbance spectra measured both in vitro and in situ showed a significant reduction of more than 90% in the amount of light-sensitive pigment in the retinas of $G^{+/+}/R^{-/-}$ mice, and ERG recordings revealed a >1 log unit loss in sensitivity. However, the histological appearances of the retinas of these mice show no significant loss of photoreceptors and little change in the lengths of their outer segments. These findings suggest that much of the ERG sensitivity loss derives from the reduced quantal absorption that results from a failure of G90D opsin to bind to its chromophore and form a normal complement of light-sensitive visual pigment. J. Comp. Neurol. 478:149–163, 2004.

Indexing terms: rhodopsin; G90D mutation; transgenic mice; retinal degeneration; stationary night blindness

Grant sponsor: National Eye Institute; Grant number: EY-10609; Grant number: EY-12190; Grant number: EY-06516; Grant number: EY-07361; Grant sponsor: Foundation Fighting Blindness (M.I.N.); Grant sponsor: Knights Templar Eye Foundation (X.-Q.D.); Grant sponsor: Oklahoma Center for the Advancement of Science and Technology (M.I.N.); Grant sponsor: U.S. Department of Veterans Affairs (N.S.P.); Grant sponsor: Alcon Research Institute (H.R.); Grant sponsor: Research to Prevent Blindness (H.R., S.J.F.); Grant sponsor: James S. Adams Scholar Award (H.R.); Grant sponsor: Senior Scientific Investigator Award (H.R.).

Ting-Huai Wu's current address is Wilmer Eye Institute, Johns Hopkins University, Baltimore, MD 21287.

*Correspondence to: Muna I. Naash, University of Oklahoma Health Sciences Center, 940 Stanton L. Young Blvd., BMSB 781, Oklahoma City, OK 73104. E-mail: muna-naash@ouhsc.edu

Received 23 March 2004; Revised 17 June 2004; Accepted 21 June 2004

DOI 10.1002/cne.20283

Published online in Wiley InterScience (www.interscience.wiley.com).

Rhodopsin, the light-sensitive pigment of rod photoreceptors, consists of the 11-*cis* aldehyde of vitamin A bound covalently to the protein opsin through a protonated Schiff-base linkage. After quantal absorption, the chromophore is converted (within a few femtoseconds) to its all-*trans* isomer (Schoenlein et al., 1991). Subsequent changes in protein conformation during the thermal decay of this molecular complex lead to the formation of an active intermediate (R*) that triggers a G-protein (transducin)-mediated enzymatic cascade and hydrolysis of cGMP. The fall in cGMP results in the closure of cationic channels in the membrane of the photoreceptor outer segment and generation of an electrical signal that is relayed across the retina to visual centers in the CNS. Defects in the molecular configuration of any component of the transduction cascade can affect the functional integrity of the photoreceptors with serious consequences for vision (cf. McLaughlin et al., 1993; Gal et al., 1994; Huang et al., 1995; Dryja et al., 1995, Danciger et al., 1995; Travis, 1998). However, the opsin apoprotein appears to be particularly susceptible to mutagenesis. More than 100 different mutations in the gene coding for the opsin moiety have been detected in patients with various forms of retinal degeneration, many of which result in night blindness, progressive constriction of the visual field, and severe visual loss (cf. Dryja et al., 1990; Humphries et al., 1992; Berson, 1993; Travis, 1998).

There are, however, three point mutations in opsin, A292E (Dryja et al., 1993), G90D (Sieving et al., 1995), and T94I (Al-Jandal et al., 1999) that have been shown to cause a form of congenital stationary night blindness (CSNB), a relatively stable disorder in which patients are night blind from early childhood, retain normal central vision, and rarely display signs of retinal degeneration except perhaps much later in life (cf. Sieving et al., 1995). Although rod sensitivity is markedly reduced, the defect in CSNB cannot be attributed to a lack of rhodopsin. Measurements of rhodopsin density and the kinetics of bleaching and regeneration in patients with various forms of CSNB closely approximate those obtained from age-matched normal subjects (Carr et al., 1966; Alpern et al., 1972; Ripps, 1982; Peachey et al., 1990; Sieving et al., 1995). However, when expressed in COS cells, the A292E, G90D, and T94I mutations were found capable of activating transducin constitutively in darkness and in the absence of 11-*cis* retinal, the rhodopsin chromophore (Dryja et al., 1993; Rao et al., 1994; Gross et al., 2003). Thus, the in vitro data suggest that, in these forms of CSNB, the mutations generate a persistent "dark light" that saturates the rod photocurrent and severely depresses rod sensitivity in much the same manner as that produced by steady background illumination.

Surprisingly, two other opsin mutations, K296E and K296M, which also exhibit constitutive activation in vitro (Robinson et al., 1994), cause autosomal dominant retinitis pigmentosa (RP) and widespread photoreceptor degeneration (Keen et al., 1991; Vaithinathan et al., 1994). The question of why different mutations, each producing a constitutively active opsin, have profoundly different consequences in terms of the nature of the disease and severity of visual loss has yet to be resolved. It has been suggested that the different phenotypes are perhaps manifestations of the same defect, where the outcome of the disease process reflects quantitative differences in the numbers of constitutively active opsin molecules contained within the photoreceptors (Dryja et al., 1993; Rao et al., 1994), but to our knowledge this possibility has yet to be explored experimentally.

Clearly, it is important to know whether a mutation at a single site in opsin can cause the phenotypes of both CSNB and RP. However, it is difficult to address this issue in humans or in an in vitro expression system, nor is it a simple matter to determine whether, in vivo, these opsin mutants are capable of binding 11-*cis* retinal to form a photosensitive pigment, as it apparently does in COS cells. These questions lend themselves to analysis in transgenic mice genetically engineered to express the mutant opsin. In this paper, we describe the creation and characterization of a transgenic mouse model carrying the G90D mutation. Data derived from histological and photochemical studies of these transgenic animals show that a range of defects results from different levels of transgene expression. Moreover, we find that expression of G90D opsin in the absence of endogenous wild-type (WT) rhodopsin, i.e., in rhodopsin knockout mice, is sufficient for formation of outer segment discs and results in electrophysiologically competent photoreceptor cells. However, despite the presence of a nearly normal complement of photoreceptors in the retinas of G90D/$R^{-/-}$ mice, electroretinographic recordings show a greater than 1 log unit loss of scotopic sensitivity, and spectrophotometric measurements indicate that their outer segments contain only ~10% of the light-sensitive pigment seen in WT retinas. Thus, the sensitivity loss appears to be due mainly to a reduction in quantal absorption that results from a failure of G90D opsin to form a normal complement of photopigment.

MATERIALS AND METHODS

Generation of G90D mice

Animal maintenance and handling conformed to the guidelines on the care and use of animals adopted by the Society for Neuroscience and the Association for Research in Vision and Ophthalmology. We constructed a G90D transgene that consisted of 15 kb of a mouse genomic fragment containing 5 kb of all opsin exons and introns as well as 6.0 kb and 3.5 kb of the 5′ and 3′ flanking sequences, respectively. In addition to the G90D substitution, several silent mutations were introduced into exon 1 by site-directed mutagenesis in a polymerase chain reaction (PCR) as described previously (Naash et al., 1993). Deleting an existing NcoI site created restriction fragment length polymorphism (RFLP) that served to distinguish between transgenic and nontransgenic mice (Naash et al., 1993). DNA isolated from 3-mm ear punches was amplified by using a set of primers that straddled exon 1 (Naash et al., 1993) and produced a 1,317-bp fragment. The PCR products were digested by NcoI to generate three fragments (197, 431, and 689 bp) from the endogenous opsin gene and two fragments (431 and 886 bp) from the transgene. Because one NcoI site in the transgene was deleted, transgenic mice had an additional 886-bp fragment (689 bp + 197 bp).

To generate founder mice, the 15-kb transgene was microinjected into 1-day-old hybrid (C57BL/6 × SJL) mouse embryos that were heterozygous for the *rd* locus (+/*rd*). Founder mice were mated to C57BL/6 mice, and transgenic offspring were identified by the presence of the NcoI

RFLP. Transgenic and nontransgenic offspring were shown to be either heterozygote or WT for the *rd* locus by analysis of the DdeI RFLP in exon 7 of the cGMP phosphodiesterase β-subunit gene (Pittler and Baehr, 1991). The *rd* locus was eliminated by outbreeding transgenic to C57BL/6 mice. Transgenic mice were mated to rhodopsin knockout mice ($R^{-/-}$; Lem et al., 1999) to express the transgene in different backgrounds of WT opsin (i.e., $R^{+/+}$, $R^{+/-}$, or $R^{-/-}$). DNA was isolated from transgenic mouse tail clippings at 3 or 4 weeks of age (Palmiter and Brinster, 1986), and the site of integration of the transgene and copy number of each founder was analyzed by Southern blot analysis. A total of 30 μg of genomic DNA was digested by EcoRI, separated on 0.6% agarose gel in TAE buffer, and transferred to a nitrocellulose membrane, and a 6 kb-fragment of the 5′ untranslated region of the transgene was radiolabeled with ^{32}P by random-primed DNA. Lines harboring more than one integration site were separated, and each site was analyzed to determine the copy number of the transgene relative to that of the endogenous gene.

Northern blot analysis and transcript quantitation

To determine the expression levels of the transgene, total RNA was isolated from the retinas of transgenic mice and normal littermates at postnatal days (P) 10, 20, and 30 by using Trizol reagent (Gibco-BRL, Gaithersburg, MD). The relative levels of transgene expression were quantified as a ratio of transgenic to WT mouse opsin mRNA (Naash et al., 1993). Total RNAs were also isolated from brain, liver, and kidney of transgenic mice to determine the tissue specificity of transgene expression. RNA samples (10 μg) were separated on a 1% agarose gel containing 18% formaldehyde. The number of retinas used to acquire this quantity of RNA ranged from two for normal mice to four for transgenic mice. The gel was stained with ethidium bromide to check the quality of the RNA (judged by the integrity of the 28s and 18s rRNA bands). The RNA was transferred to nitrocellulose membrane and hybridized with a mutant primer MIN 124 (5′-GGT*C*GT*C*GTAAA*AT*CTC) specific for the transgene transcripts; the probe contained five nucleotide modifications that allowed differentiation of the mutant and endogenous transcripts. The blots were then stripped and subsequently reprobed with the normal primer MIN 125 (5′-GGGTGGTGGTGAATCCTCC) that recognizes only the transcripts formed by the endogenous opsin gene. MIN 124 and 125 were gel purified and end labeled with [γ-^{32}P]ATP in the presence of T4 polynucleotide kinase. The relative amounts of RNAs in the blots were examined by reprobing with cyclophilin cDNA. Hybridization was performed at 37°C for 24 hours in a medium containing 40% formamide, 5× Denhardt's solution, 5× standard saline citrate (SSC), 10% dextran sulfate, 50 mM sodium phosphate (pH 6.8), 0.1% sodium dodecyl sulfate (SDS), 0.5 mg/ml denatured salmon sperm DNA, and 2×10^6 CPM/ml end-labeled oligonucleotide (Naash et al., 1993). The blots were washed with 2× SSC containing 0.2% SDS and again with 0.5× SSC containing 0.2% SDS at 37°C. They were then exposed at –70°C to Kodak XAR film between two intensifier screen, and densitometric scans were obtained from each band; the averages of three measurements were obtained and normalized with respect to the amount of cyclophilin in the corresponding lane. RNA slot blot analyses were also performed to quantitate the levels of transgene expression in total retinal RNA isolated from 15-day-old transgenic and normal littermates. The blots were spotted with serial dilutions of RNA ranging from 0.1 to 10 μg. The blots were treated as indicated above, and the expression levels of the transgene were compared with the level of the normal. The values were normalized to the amount of cyclophilin in the corresponding sample.

Histology and immunocytochemistry

Animals were killed by carbon dioxide, and the superior cornea was marked prior to enucleation for subsequent orientation. A full-thickness incision was made in the cornea, and the globe was immersed for 1 hour at 4°C in "mixed aldehyde" fixative, containing 2% paraformaldehyde, 2.5% glutaraldehyde, and 0.1 mM $CaCl_2$ in 0.1 M sodium cacodylate buffer, pH 7.4. After removing most of the anterior segment, the eyecup was kept in fixative overnight at 4°C. The posterior portion of each eye was then divided along the vertical meridian so that each half contained the superior and inferior quadrants of either the nasal or the temporal retina. The tissue was then postfixed in osmium tetroxide, dehydrated through a graded series of ethanols, embedded in epoxy resin (Epon), and prepared for light microscopy (LM) and electron microscopy (EM). For LM, sections (1 μm thick) were cut through the optic nerve head approximately along the vertical meridian and stained with methylene blue-azure II. Photoreceptor nuclei were counted in a microscopic field that spanned 225 μm and was centered at 300 μm from the edge of the optic nerve head; except where indicated, the histological sections and cellular measurements were performed on the superior retina. Single eyes from three mice, taken from separate litters, were used for each postnatal age evaluated. Thin sections (~0.1 μm) for EM were cut on a diamond knife, collected on uncoated copper mesh grids, and stained with uranyl acetate and lead citrate. Sections were examined and photographed in a Zeiss 10CA (Carl Zeiss, Oberkochen, Germany) electron microscope.

Opsin localization was visualized at the LM and EM levels by immunocytochemical labeling of retina sections with rabbit anti-bovine opsin IgG. This antibody had been used previously to label normal opsin (Tan et al., 2001). For EM immunogold labeling, sections were processed essentially as described by Tan et al. (2001). Prior to embedment, eyecups that had been fixed with mixed aldehydes were rinsed briefly through several changes of 0.1 M sodium cacodylate buffer, pH 7.4, then treated with 0.15 M glycine in the same buffer for 30 minutes at 4°C (to quench free aldehyde groups, and rinsed again several times with cacodylate buffer. Embedment in LR white resin (Electron Microscopy Sciences, Fort Washington, PA) followed the method of Erickson et al. (1993), using dehydration through a graded methanol series and en bloc staining with 2% uranyl acetate at the 70% methanol stage. For EM immunogold labeling, thin sections (silver-gold) were placed onto uncoated nickel grids and treated for 15 minutes at room temperature with 50 mM ammonium chloride, followed by blocking for 30 minutes at room temperature with phosphate-buffered saline [PBS; 0.1 M sodium phosphate, pH 7.4, containing 0.9% (w/v) NaCl] containing 1% (w/v) radioimmunoassay (RIA)-grade bovine serum albumin (BSA), 10% (v/v) normal goat serum,

and 0.05% (v/v) Triton X-100. Grids were exposed overnight at 4°C either to rabbit anti-bovine opsin IgG (Tan et al., 2001) or to nonimmune rabbit serum (each diluted 1:250 with blocking buffer), then rinsed briefly with PBS and treated for 2 hours at room temperature with goat anti-rabbit IgG conjugated to 10-nm colloidal gold (AuroProbe EM GAR G10; Amersham, Arlington Heights, IL; diluted 1:50 with blocking buffer). After being rinsed briefly with PBS, sections were treated with 1% glutaraldehyde (5 minutes at room temperature), then rinsed serially with PBS and distilled water, stained with uranyl acetate and lead citrate, rinsed again with distilled water, exposed to OsO_4 vapors, and air dried. Sections were viewed with a Jeol JEM-1200EX electron microscope at an accelerating voltage of 80 KeV.

For LM immunolabeling, thick sections (0.75 μm) of LR white-embedded retinas on glass slides were treated essentially as described above for thin (EM) sections, except the primary antibody (or nonimmune control serum) was diluted 1:500 (v/v) with blocking buffer and incubation was carried out for 2 hours at room temperature. After being rinsed briefly with PBS, sections were treated for 2 hours at room temperature with 1-nm colloidal gold-conjugated goat anti-rabbit IgG secondary antibody (AuroProbe7 One GAR; diluted 1:50 (v/v) with blocking buffer). Sections were rinsed three times (15 minutes each) with PBS, followed by fixation for 10 minutes at room temperature with 2% (v/v) glutaraldehyde in PBS and then were rinsed with distilled water (twice, 5 minutes each). Silver intensification was performed with an IntenSE7 M Silver Enhancement Kit, per the directions of the manufacturer. Sections were then rinsed with distilled water, counterstained with 1% (w/v) toluidine blue in 1% (w/v) sodium borate, rinsed again with distilled water, air dried, and coverslipped using Permount7. Sections were viewed and photographed with an Olympus BH-2 photomicroscope in the autoexpose mode, using a ×20 DplanApo objective.

Retinal densitometry

In situ measurements of retinal absorbance were made with a microscope-based transmission densitometer that was modified for computer analysis (Ripps and Snapper, 1974) from the rapid scan fundus reflectometer designed by Weale (1953). The retina was removed from a dark-adapted mouse for over 24 hours under deep red illumination, placed receptor side up on a glass slide mounted on an X-Y stage, and positioned with an infrared viewing device in the path of the measuring beam. Light that had passed sequentially through a series of interference filters (wavelengths from 400 to 700 nm) was directed by a high-transmission fiber optic bundle to the underside of the glass slide, traversed the isolated retina as a collimated beam 1.5 mm in diameter centered ~1 disc diameter from the optic nerve head, and was incident upon the face a sensitive photomultiplier, the output of which was digitized, recorded, and analyzed off line. Absorbance difference spectra $[\Delta D]_\lambda$ represent the wavelength variation in retinal transmission between scans recorded from a dark-adapted retina, and again after the retina had been exposed for 2 minutes to an intense yellow light (Wratten 16; 4.63×10^2 μW mm^{-2}) that bleached virtually the full complement of available rhodopsin in the test area of the measuring beam. It is important to note that the values of $[\Delta D]_\lambda$ are not an accurate indicator of rhodopsin density for light passing axially through the ROS. The measured absorbance changes are diluted by that fraction of the light reaching the photocell that has passed through the interstices between photoreceptors (stray light) and, in the case of the isolated retina, by disorientation of receptor outer segments with respect to the path of the incident light. Nevertheless, reliable measurements can be obtained by averaging data from several retinas of the same genotype, and the technique provides a valid means by which to compare the relative content of rhodopsin in normal and diseased retinas (Goto et al., 1995).

ROS membrane isolation, Western blot analyses, and spectrophotometry

Retinas were isolated from dark-adapted animals for over 24 hours, and ROS membranes were purified in discontinuous sucrose density gradients, as described by Fung (1983). Retinas were placed in buffer A [20 mM NaCl, 60 mM KCl, 2 mM $MgCl_2$, 1 mM dithiothreitol (DTT), 0.1 mM phenylmethylsulfonyl fluoride (PMSF), and 10 mM MOPS, pH 7.5] with 26% (w/v) sucrose. ROS membranes were released from retinas by repeated passage of the tissue through the orifice of a pipette. To each 11- × 60-mm centrifuge tube, 0.5 ml of the resulting suspension was layered gently on top of a discontinuous gradient containing 0.7 ml buffer A with 26% w/v sucrose on top of 3 ml buffer A with 40% w/v sucrose. After centrifugation for 30 minutes at 140,000*g* at 4°C (SW 60 rotor; Beckman Instruments, Inc., Carlsbad, CA), ROS membranes were collected from the interface of the 26% and 40% sucrose solutions. They were then washed and suspended in buffer A. Protein concentration was determined by the method of Lowry (1951).

ROS membrane proteins were separated by 10% SDS-polyacrylamide gel electrophoresis (PAGE) and transferred to nitrocellulose. Gels for Western blots contained ~20 μg protein per lane. Western blots were blocked with TBST buffer containing 5% (w/v) nonfat milk and incubated with a 1:1,000 dilution of a monoclonal antibody (mAb) 1D4, an anti-bovine rod opsin antibody. This mAb, which is specific for the C-terminus of rod opsin (Hodges et al., 1988), was provided by Dr. R. Molday and had been used previously to label normal opsin and opsins with mutations on the extracellular/intradiscal surface (see, e.g., Olsson et al., 1992; Wu et al., 1998). Opsin was visualized after incubation with anti-mouse IgG conjugated to horseradish peroxidase (HRP) and enhanced chemiluminescence (Amersham ECL kit). The blot was incubated in detection solution for 1 minute and then exposed to a Biomax film (Kodak) for 2 minutes. The intensity of opsin labeling was determined by densitometry (BioImage Intelligent Quantifier). Data were obtained from three separate experiments, each using both retinas from three control and three G90D mice on different opsin genetic backgrounds.

Levels of rhodopsin in ROS preparations from G90D and normal mice were determined spectrophotometrically. ROS membranes were solubilized in 20 mM Tris buffer, pH 7.0, containing 1% (w/v) polyoxyethylene 10 tridecyl ether (Emulphogene; Sigma, St. Louis, MO) and 20 mM hydroxylamine (NH_2OH); particulate matter was removed by centrifugation at 7,000*g* for 10 minutes. Absorbance spectra were recorded from the ROS samples (Perkin-Elmer model 48 spectrophotometer) before and after exhaustive bleaching.

Absorbance measurements on retinal extracts

The procedure for obtaining spectrophotometric measurements on retinal extracts has been described previously (Williams et al., 1998; Sieving et al., 2001). Briefly, retinas removed from mice that had been dark adapted overnight were added to 400 μl distilled water and macerated in a manual tissue grinder, and, after two washes in distilled water, the solution was centrifuged at 10,000*g* for 10 minutes. The supernatant was discarded, and 1 ml of Tris buffer (20 mM, pH 6.5) containing 1% polyoxyethylene 10 tridecyl ether (Emulphogene; Sigma) was added to the pellet. The pellet was disrupted with a spatula and the solution gently agitated for 1 hour at 4°C. After 10 minutes of centrifugation at 10,000*g*, the supernatant was withdrawn, transferred to a cuvette, and scanned (260–800 nm) with a Cary 300 spectrophotometer. The solution was then bleached completely by using a microscope illuminator for 2 minutes and then rescanned, and the bleaching difference spectra were calculated.

Electroretinography

After overnight dark adaptation, mice were anesthetized with ketamine (80 mg/kg) and xylazine (16 mg/kg), and the pupils were dilated with eye drops (1% tropicamide, 2.5% phenylephrine HCl, 1% cyclopentolate HCl). The mice were placed on a regulated heating pad, and ERGs were recorded with a stainless-steel wire electrode that made contact with the corneal surface through a layer of methylcellulose. Platinum needle electrodes placed in the cheek and tail served as reference and ground leads, respectively. Responses were differentially amplified (1–1,500 Hz), averaged, and stored with a LKC UTAS E-3000 signal averaging system.

Dark-adapted ERGs were recorded to stimulus flashes ranging from 0.001 to 137 cd second/m^2. The amplitude of the a-wave was measured from the prestimulus baseline to a specific time point (8 msec) after stimulus onset.

RESULTS

Generation of transgenic mice

Figure 1A shows construction of the G90D transgene, which consisted of a 15-kb fragment of the mouse opsin gene with 6 kb of the 5′ promoter region. The three fragments (197, 431, and 689 bp) generated from NcoI digestion of the PCR product generated from the endogenous opsin gene and the two fragments (431 and 886 bp) derived from the transgene are shown in Figure 1B. Injection of the G90D construct produced 10 potential founders (F_0) that were identified by the presence of the NcoI RFLP (Fig. 1C). Eight of the founders passed the transgene to their offspring at 50% transmittance (Mendelian inheritance) and expressed the transgene at different levels. Permanent lines of G90D transgenics were generated from each founder, and the transgene was moved into different backgrounds of the WT allele ($R^{+/+}$, $R^{+/-}$, and $R^{-/-}$) by appropriate crossings with rhodopsin null mice ($R^{-/-}$; Lem et al., 1999). Southern blot analyses were performed on all lines to isolate different integration sites and to determine copy numbers of the transgene (data not shown); the copy numbers in the three lines (G_{86}, G_{45}, and G_{41}) that we characterized were 1, 4, and 6, respectively.

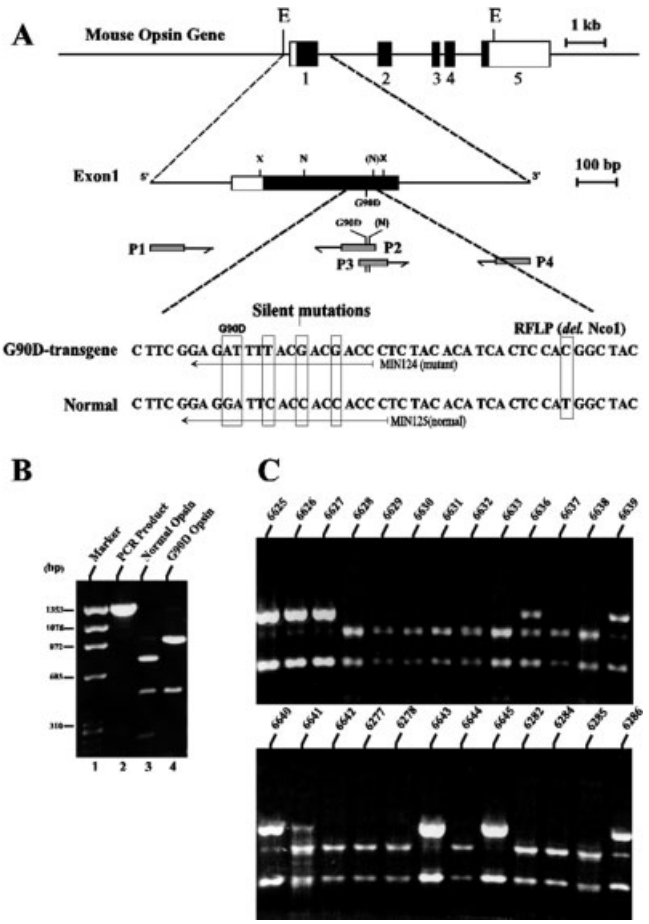

Fig. 1. Generation of the G90D mutation and identification of potential founder mice. **A:** The uppermost row shows a map of the mouse opsin gene (15 kb) containing the five exons encoding opsin (solid rectangles numbered 1–5). Exon 1 of the transgene with relevant restriction sites and introduced RFLP (deletion of NcoI) are shown in the middle row. Symbols representing the restriction sites are X = XhoI; N = NcoI; (N) = deleted NcoI site. Rectangles highlight the changes in the nucleotide sequence to introduce the G90D, silent, and RFLP mutations in the transgene. P1, P2, P3, and P4 are primers used for PCR amplification and mutagenesis. **B:** Ethidium bromide-stained agarose gel showing the amplified transgene product (lane 2) and the NcoI-digested PCR product from normal (lane 3) and transgenic (lane 4) opsin. See text for details. **C:** Ethidium bromide-stained agarose gel showing NcoI digestion pattern of PCR products amplified from extracted tail DNA from 25 potential founders, 10 of which contain the transgene.

Expression of the transgene

Mutant oligonucleotide (MIN 124), containing the six nucleotide modifications shown in Figure 1A, was used as a probe to distinguish the mutant from the endogenous transcripts in the three lines studied; normal oligoneucleotide (MIN 125) was used as a probe to differentiate the WT transcripts from the transgenic. As shown in Figure 2A, the mutant probe hybridized only to the mutant transcripts, whereas the normal probe hybridized only to normal transcripts. Five transcripts with molecular sizes of 1.7, 2.2, 3.1, 3.9, and 5.1 kb were identified in all lines when the blot was hybridized with the ^{32}P-labeled mutant or normal primer, indicating that the transgene is coex-

pressed with the endogenous opsin gene. Furthermore, the mutant transcripts have the same mobility as the WT mouse opsin gene (Al-Ubaidi et al., 1990), indicating that the transgene was transcribed and processed correctly. No bands were detected in RNAs isolated from brain, liver, and kidney from line G_{86}, indicating that the transgene was expressed solely in the retina (Fig. 2A). Quantitative analysis of transgene expression showed that the ratio of transgenic to normal RNA for lines G_{86}, G_{45}, and G_{41} was 0.5:1, 1.7:1, and 2.5:1, respectively; the data are based on three independent RNA slot blot measurements from 15-day-old retinas isolated from normal and transgenic mice. The mice are identified in subsequent sections as $G_{0.5}$, $G_{1.7}$, and $G_{2.5}$ to reflect the transgene expression level.

Figure 2B shows Western blot data obtained from retinal extracts of 1-month-old $G_{0.5}$, $G_{1.7}$, and $G_{2.5}$ mice on the $R^{+/+}$ and $R^{-/-}$ backgrounds. The upper panel illustrates the blot probed with mAB 1D4 in which the opsin monomer, dimer, and higher order aggregates were detected in lanes 1–3 (transgenics in the WT background). The absence of aggregates in the last three lanes is due largely to the lower levels of opsin protein in photoreceptors with fewer and shorter outer segments, a reflection of transgene expression in the different lines; e.g., the advanced degenerative state of the $G_{2.5}{}^{+/-}/R^{+/+}$ retina. Note, however, that both the $G_{0.5}$ and the $G_{1.7}$ retinas on the $R^{-/-}$ background contain relatively normal amounts of peripherin/*rds* and Rom-1 proteins. Opsin levels, determined from six individual samples of Western blots and corrected for protein loading and peripherin/*rds* expression (an index of outer segment protein content), enabled us to calculate the percentage of opsin relative to that found in WT retinas (see Materials and Methods). Opsin levels in $G_{0.5}{}^{+/-}/R^{+/+}$ retinas were equivalent to those of WT, whereas the other two lines show protein expression greater than in WT (~142% and 220% of WT for $G_{1.7}$ and $G_{2.5}$, respectively). In contrast, G90D protein levels for the two lines studied on the $R^{-/-}$ background were ~24% and 30% of WT amounts in $G_{0.5}$ and $G_{2.5}$, respectively. Comparing the transgene expression levels with the amounts of protein formed in the two genetic backgrounds showed no correlation. Clearly, the sites of integration of the transgene, the coregulation of the mutant and endogenous genes, and the copy number of the transgene are factors that dictate the level of transgenic opsin that is formed (cf. Tan et al., 2001).

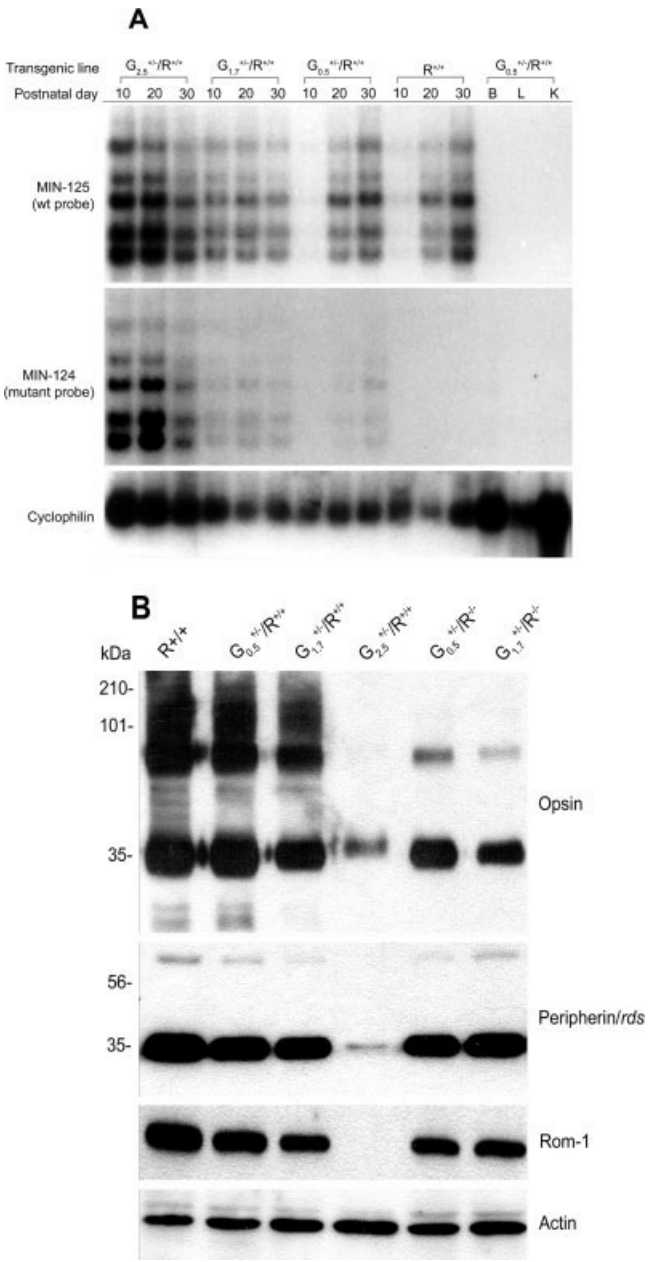

Fig. 2. Expression of the G90D transgene. **A:** Northern blot of total RNAs isolated from transgenic and normal mice at P10, P20, and P30 and total RNAs isolated from the brain (B), liver (L), and kidney (K). Lanes 1–3: $G_{2.5}$; lanes 4–6: $G_{1.7}$; lanes 7–9: $G_{0.5}$; lanes 10–12: $R^{+/+}$; lanes 13–15: B, L and K. Autoradiograms of the upper blot were hybridized with WT probe (MIN 125), the middle with mutant probe (MIN 124), and the lower with cyclophilin to control for RNA loading. **B:** Western blot analysis of retinal extracts isolated from WT and transgenics from three lines on the $R^{+/+}$ and $R^{-/-}$ backgrounds. The upper blot was reacted with mAb 1D4; the middle two blots were immunoreacted with peripherin/*rds* and Rom-1 antibodies to control for photoreceptor degeneration; the lower blot was probed with an actin antibody to control for protein loading.

Structural characterization of the G90D retina on the WT background

Retinal structure in three transgenic lines. We observed a direct relation between the level of transgene expression and the extent of photoreceptor degeneration. Histological sections of retinas from 1-month-old animals representing each of the three G90D transgenic lines on the WT background expressing two endogenous rhodopsin alleles ($R^{+/+}$) and from a nontransgenic littermate are shown in Figure 3A. The light micrographs (upper panel) show no obvious signs of abnormalities in the retinas of $G_{0.5}{}^{+/-}/R^{+/+}$ animals, the line with the lowest level of transgene expression, approximately equivalent to one WT allele. The length and organization of the photoreceptor inner and outer segments as well as the thickness of the outer nuclear layer (ONL) were similar to normal. When transgene expression was approximately 1.7- and 2.5-fold greater than that produced by the WT gene ($G_{1.7}$ and $G_{2.5}$ mice, respectively), there were significant changes in retinal structure by 1 month of age. In $G_{1.7}{}^{+/-}/R^{+/+}$ mice, the inner/outer segment length was about 62%

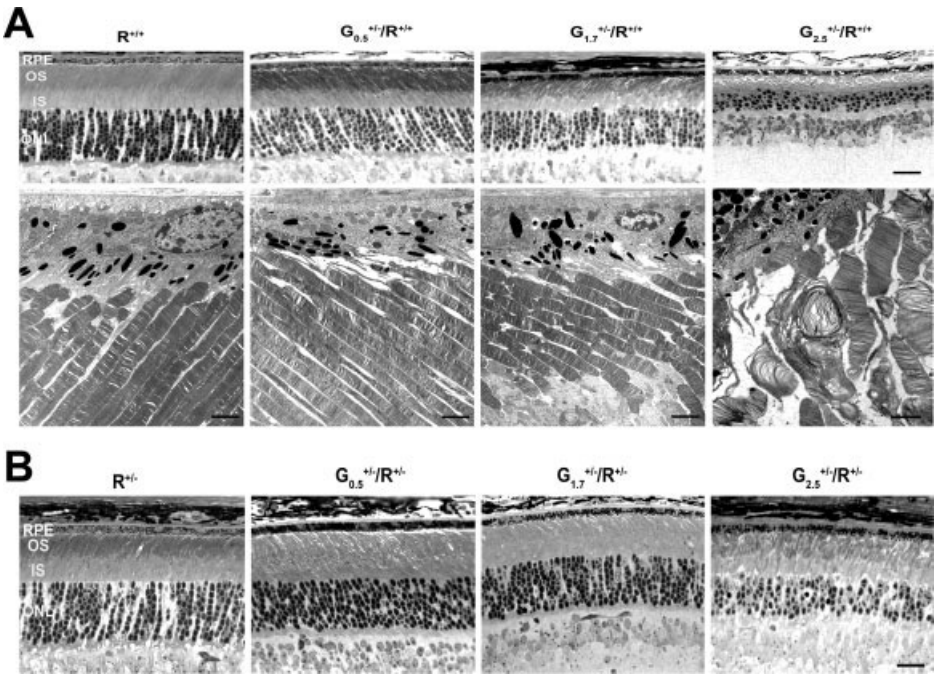

Fig. 3. Histology and ultrastructure of transgenic retinas at 1 month of age. **A:** Light microscopic (upper panels) and electron microscopic (lower panels) appearance of the retinas from three lines ($G_{0.5}$, $G_{1.7}$, and $G_{2.5}$) of transgenic mice in the $R^{+/+}$ background. At this age, the outer nuclear layer (ONL) of the $R^{+/+}$ retina typically contains about 10 or 11 rows of nuclei, and the photoreceptors display closely packed, well-organized inner and outer segments. Retinal sections of 1-month-old $G_{0.5}$ mice appeared similar to normal. For their $G_{1.7}$ littermates, inner/outer segment length was about 62% of normal, and the thickness of the ONL was reduced to approximately seven rows of nuclei. In the $G_{2.5}$ mice, the photoreceptors appeared disorganized and disrupted, and there was a greater reduction in the nuclear content of the ONL. **B:** Light microscopy of the same transgenic lines on the $R^{+/-}$ background. The absence of one copy of the WT allele improved the histological appearance of the $G_{1.7}$ retina, but, because of opsin overexpression, it had little effect on the $G_{2.5}$ retina. RPE, retinal pigment epithelium; OS, outer segment; IS, inner segment; ONL, outer nuclear layer; INL, inner nuclear layer. Scale bars = 20μm in A (upper panels),B; 2.6 μm in A (lower panels).

of normal, and the thickness of the ONL was reduced by the loss of two or three rows of nuclei. In $G_{2.5}{}^{+/-}/R^{+/+}$ mice, there was a further shortening of the outer segments, a greater reduction in the nuclear content of the ONL, and signs of disorganized inner and outer segments. The electron micrographs (lower panel) of the photoreceptor/RPE interface from animals of comparable age (Fig. 3A) show the normal appearance of the photoreceptors in $G_{0.5}$ mice, the early ultrastructural changes in $G_{1.7}$ mice, and the severe disruption of cellular integrity in $G_{2.5}$ transgenics.

In patients carrying the G90D mutation, one copy of the transgene is expressed together with one copy of the WT allele. To mimic this situation, we moved our transgenic mice into the $R^{+/-}$ genetic background, thereby reducing the total level of endogenous opsin expression. We observed no significant changes in the histological appearance of the $G_{0.5}$ and $G_{1.7}$ retinas for a period of several months, whereas the $G_{2.5}$ retina showed signs of degeneration as early as 1 month of age (Fig. 3B). It appears likely that eliminating one WT allele from the $G_{1.7}$ line had a beneficial effect on retinal structure; the persistent degeneration in the $G_{2.5}$ line suggests that opsin overexpression was probably still a factor. These results provide strong evidence that overexpression of the G90D transgene induces early-onset retinal degeneration, a situation seen previously in mice overexpressing the WT opsin gene (Olsson et al., 1992; Tan et al., 2001).

Age-related morphological changes in the $G_{0.5}$ retina. To eliminate the effects of opsin overexpression on the G90D-associated retinal phenotype, the subsequent experiments were performed on the $G_{0.5}$ line. Figure 4A shows a series of LM images of retinas from 6-month-old WT and from 2-, 3-, 4-, 7-, and 9-month-old $G_{0.5}$ mice. It should be noted that, up to 3 months of age, the retinas of $G_{0.5}{}^{+/-}/R^{+/+}$ mice appeared quite normal; the ONL contained 10 or 11 rows of nuclei, and the lengths of the inner/outer segments were within normal limits. In contrast, histological sections of older animals showed evidence of age-related pathological changes. By 4 months of age, there was a loss of about two rows of nuclei and a shortening of the ROS. Over the next 5 months, there was a progressive loss of photoreceptor nuclei and further shortening of the inner/outer segments, but the cells seemed relatively well organized, and there was a clear demarcation between inner and outer segments. Figure 4B presents a quantitative analysis of the numbers of photoreceptor nuclei and inner/outer segment lengths taken from measurements obtained in a 225-μm width of a segment of the superior and inferior retina located ~300 μm from the edge of the optic nerve. The averaged data (±SD) were obtained from six to eight retinas at 1, 4, and 7 months of age. There was a consistent, but insignificant, reduction in both metrics even at 1 month of age. At 4 and 7 months of ages, the reduction was more evident and was

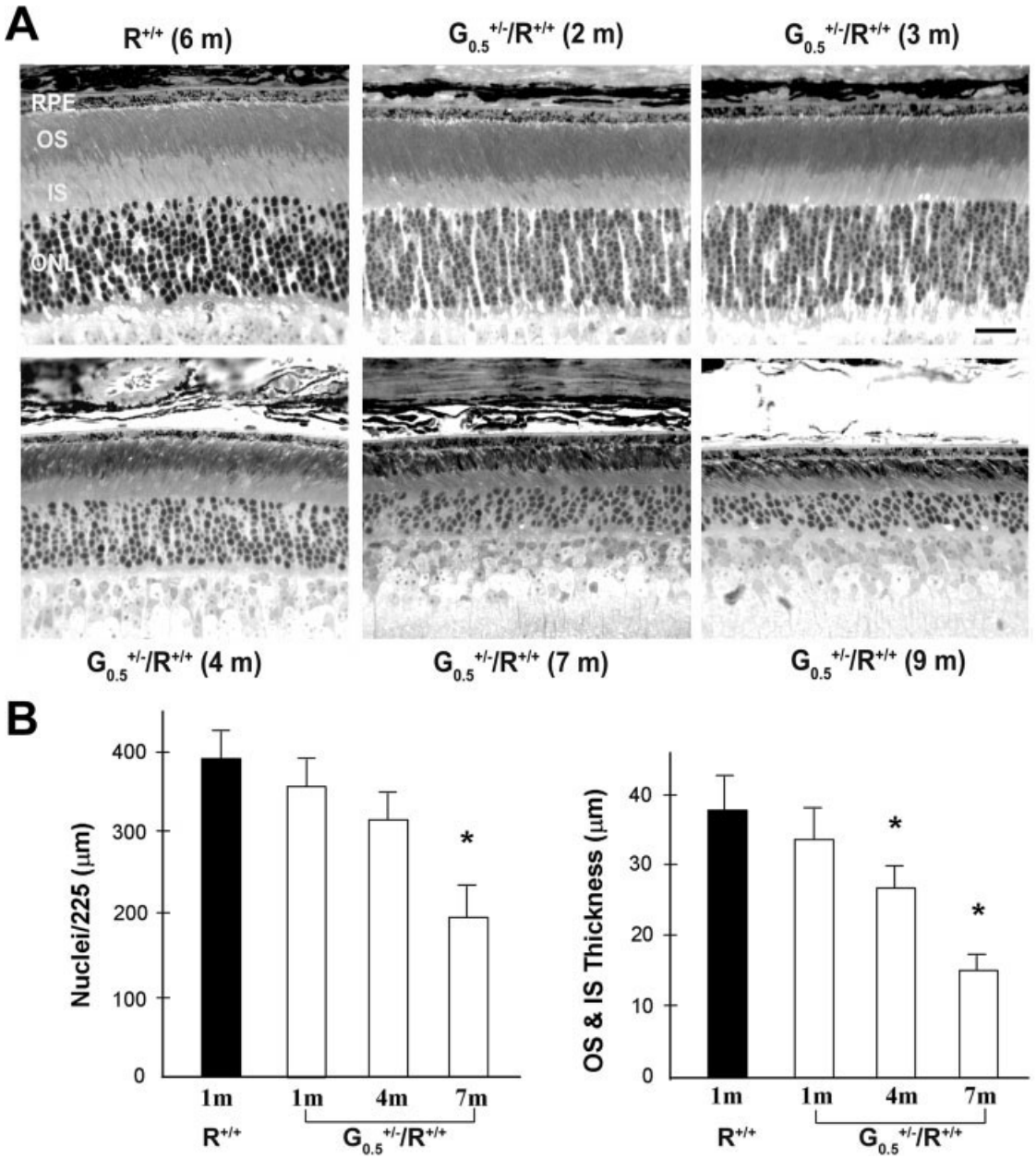

Fig. 4. Age-related morphological changes in $G_{0.5}^{+/-}$ mice. **A:** Light micrographs showing the normal appearance of the transgenic retina up to 3 months of age, and the gradual loss of visual cells thereafter. **B:** Bar graphs illustrating the results of quantitative analysis of the nuclear content and outer segment/inner segment lengths as a function of age. See text for details. Significant difference ($P < 0.05$, student's t test) between transgenics and non-transgenics are marked with asterisks. Scale bar = 28 μm.

statistically significant ($P = 0.0085$ and $P = 0.0012$, respectively).

When two copies of the $G_{0.5}$ transgene were present ($G_{0.5}^{+/+}/R^{+/+}$), defects in retinal structure were more severe and seen at earlier ages. The EM images in Figure 5 show relatively compact outer segment structure at 2 months of age, although early signs of morphological defects are apparent. By 4 months, there are disoriented outer segment membranes (Fig. 5, arrowheads), and, at 9 months, many of the ROS were severely disrupted and contained large vacuoles (Fig. 5, asterisk).

Structural characterization of the $G_{0.5}$ retina on the rhodopsin knockout background

Retinal structure of $R^{-/-}$ mice shows a normal complement of rod nuclei at early postnatal stages, but the cells fail to form ROS, and amorphous remnants of the inner segments fill the subretinal space (Fig. 6A). Without the structural protein opsin, there is a progressive loss of photoreceptors, and, by the time the animals are 3 months of age, the ONL is reduced to a single row of nuclei that

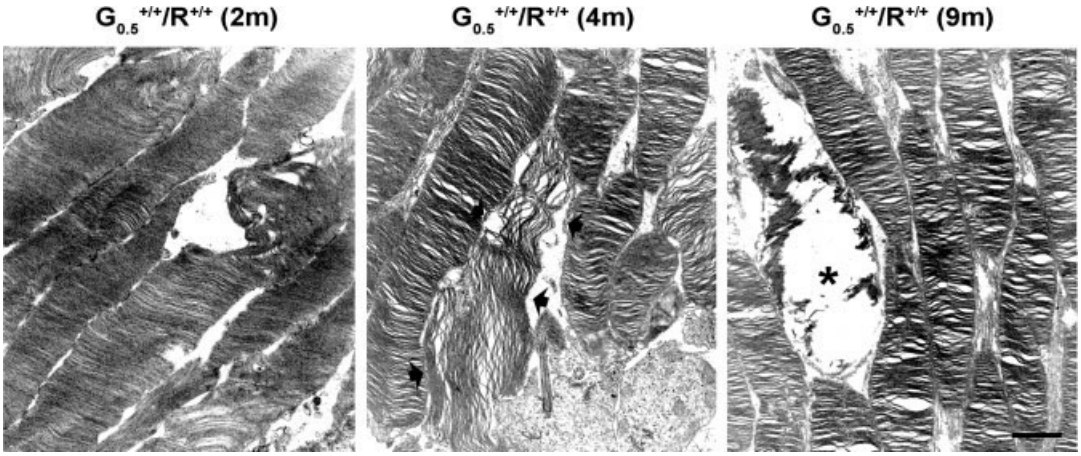

Fig. 5. Ultrastructural images of $G_{0.5}^{+/+}/R^{+/+}$ mice. With the addition of another mutant allele, there are early signs of morphological defects. By 4 months, outer segment membranes are disoriented (arrowheads), and, at 9 months, many of the ROS are disrupted and contained large vacuoles (asterisk). Scale bar = 1 μm.

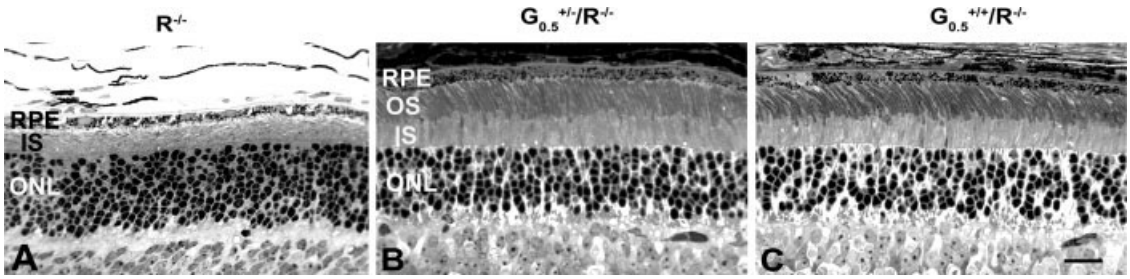

Fig. 6. Light micrographs of the 1-month-old rhodopsin knockout retina ($R^{-/-}$) and $G_{0.5}$ hetero- and homozygotes on the opsin null background. **A:** $R^{-/-}$ mice show a normal complement of rod nuclei, but lack outer segments. Note the amorphous structure of the subretinal space. **B:** Introducing the $G^{+/-}$ mutation resulted in an increased formation of photoreceptors, the development of ROS, and prolonged survival of photoreceptors. **C:** A similar effect was seen when two copies of the transgene were placed on the null background. Scale bar = 24 μm.

are predominantly the cell bodies of cone photoreceptors (cf. Humphries et al., 1997; Lem et al., 1999; Jaissle et al., 2001). However, Sieving et al. (2001) have shown that introducing one allele of their G90D transgene into the $R^{-/-}$ background provides the structural protein required for outer segment development and enhances rod survival; indeed, homozygous transgenic mice ($G^{+/+}/R^{-/-}$) showed little evidence of cell loss even at 1 year of age. We observed a similar "rescue" effect of the G90D opsin used in this study, although inclusion of the transgenic opsin was less effective, and cell survival showed significant regional variation. The retinal section in Figure 6B shows how incorporation of one copy of the transgene in the null background ($G^{+/-}/R^{-/-}$) resulted in the development of ROS and prolonged survival of photoreceptors in the superior region of the central retina of 1-month-old mice. A similar effect with equally good photoreceptor preservation was seen when two copies of the transgene were placed on the null background (Fig. 6C). However, sections from regions of the inferior retina gave very different results. Although expressing one allele of the $G_{0.5}$ transgene on the null background induced the elaboration and maturation of ROS in the central superior (CS) retinas of 4-month-old mice (Fig. 7A), there were far fewer photoreceptors in the central inferior (CI) region of the same retina (Fig. 7B). By 10 months of age, the CS retina showed remarkably good structural integrity (Fig. 7C), but there was a marked and significant ($P = 0.01$) degree of photoreceptor degeneration in the CI region of the same retina (Fig. 7D). The greater susceptibility of the inferior retina to degenerative changes is not uncommon in transgenic animals and humans carrying mutations in opsin (Naash et al., 1993, 1996; Garriga and Manyosa, 2002; Stojanovic and Hwa, 2002). However, it is not clear why this predilection should be so pronounced when the G90D protein substitutes for WT protein to support the formation and development of outer segment membranes.

Cellular localization of G90D opsin

The question of whether the mutant G90D protein is translocated from sites of synthesis in the rod inner segment to the disc membranes of the outer segment was examined via LM and EM immunochemistry using rabbit anti-bovine opsin polyclonal antibody that recognizes both WT and mutant opsin. Extensive labeling of the reaction product localized to the ROS and the distribution of immunogold particles throughout the disc membranes of WT mice are shown in Figure 8A and D, respectively. In con-

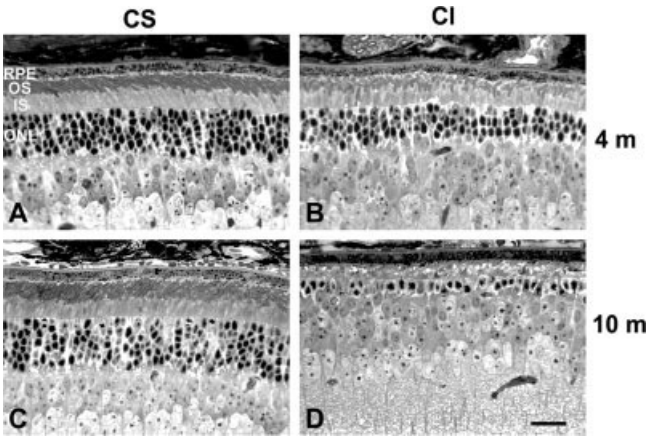

Fig. 7. Regional differences in the rate of photoreceptor degeneration in the central superior (CS) and central inferior (CI) areas of the $G_{0.5}^{+/-}/R^{-/-}$ retinas at 4 (**A,B**) and 10 months (**C,D**) of age. At both ages, the superior retina showed better structural integrity compared with the inferior retina. Note that, at 10 months, the superior retina continues to show reasonably good cellular morphology, whereas the inferior retina is grossly abnormal. See text for details. Scale bar = 40 μm.

trast, no labeling is seen in either the inner nuclear layer or the cellular debris at the photoreceptor/RPE interface of $R^{-/-}$ mice (Fig. 8B,E), a strong evidence that, as expected, no WT protein is formed in the rhodopsin knockout retina. Thus, the antibody labeling of the outer segments of $G_{0.5}^{+/+}/R^{-/-}$ mice (Fig. 8C,F) indicates that G90D opsin has been properly localized and integrated into the ROS disc membranes.

Functional analysis

The presence of G90D opsin in the ROS of transgenic animals does not ensure that it is able to bind the 11-*cis* chromophore to form a functional (i.e., light-sensitive) photopigment. To address this issue, absorbance spectra were measured on rhodopsin extracts of isolated ROS, on whole retinal extracts, and on intact retinas removed from the eyecups of WT and transgenic mice. In addition, the response properties and photic sensitivity of the retina were determined from ERG recordings to a range of flash intensities.

Rhodopsin extracts. Figure 9A shows absorbance spectra recorded before and after exposure to an intense bleaching light from ROS extracts in which 30 μg of protein was used for each set of measurements; Western blot analysis of ROS samples immunoreacted with mAb 1D4 (Fig. 9B) show that, except for aliquots from the $R^{-/-}$ sample, nearly equivalent amounts of opsin protein were used for the absorbance measurements. The records were obtained from 3-week-old WT and $G_{0.5}^{+/-}$ animals on different backgrounds; at this age, there is relatively little photoreceptor degeneration in transgenics on the $R^{+/+}$, $R^{+/-}$, or $R^{-/-}$ backgrounds (see Figs. 3, 7). The light-induced absorbance changes (ΔAbs) presented in each panel show that the presence of the G90D transgene, whether on the $R^{+/+}$ or on the $R^{+/-}$ background, reduced the amount of photolysable rhodopsin. Moreover, no bleachable pigment was detected in the transgenic and nontransgenic littermates on the $R^{-/-}$ background.

The absence of a measurable amount of light-sensitive pigment when the G90D protein is extracted from ROS of $G_{0.5}^{+/-}/R^{-/-}$ mice may be attributable to the use of hydroxylamine (see Materials and Methods), an agent that has been shown to release 11-*cis* retinal from the G90D protein in the absence of light (Sieving et al., 2001). To circumvent this problem, spectroscopic measurements were performed on whole retinal extracts in the absence of hydroxylamine. Figure 9C presents pooled data from two sets of measurements, each of which was obtained from five WT, four $G_{0.5}^{+/+}/R^{-/-}$, and four $G_{0.5}/R^{-/-}$ retinas. After correcting for the number of samples in each data set, the average absorbance values for WT and $G_{0.5}^{+/+}/R^{-/-}$ are 0.0124 and 0.00125, respectively. Thus, it appears that, even in the absence of hydroxylamine, the G90D protein forms only a small quantity of bleachable pigment, approximately 10% of the WT.

In situ measurements. Because of the very low level of photopigment found in retinal extracts, we considered the possibility that the binding of 11-*cis* retinal to the G90D protein is so weak that the complex was dissociated during the isolation procedure. To address this issue, we measured bleaching difference spectra on whole amounts of isolated intact retinas. Figure 10 shows absorbance measurements from isolated retinas of various genotypes. The data represent the absorbance differences obtained from spectral scans acquired before and after exposure to illumination that bleached virtually all rhodopsin molecules in the measuring field. A pairwise comparison of the panels reveals some important features of the G90D mutation. In WT animals (Fig. 10A) the averaged value for the density difference at the λ_{max} of ~510 nm was 0.132. With the addition of one copy of the G90D allele (Fig. 10B), the absorbance diminished by about 20%, to 0.106, suggesting a down-regulation of WT rhodopsin expression or interference with its normal rate of regeneration. Furthermore, there is no evidence of a contribution of the G90D opsin to the bleaching difference spectrum. A similar phenomenon is seen in the next set of data. Figure 10C shows the results for heterozygotes ($R^{+/-}$) in which the presence of only one copy of the WT allele reduced the absorbance measurements by ~36%, to 0.084; with the addition of the G90D allele (Fig. 10D), there was a further reduction to 0.068 absorbance units. Further evidence that the G90D protein does not bind effectively to the chromophore in vivo is seen in the last set of data in which the G90D mutation was placed on the $R^{-/-}$ background. As shown in Figure 10E, the retina of the $R^{-/-}$ mouse contains no bleachable rhodopsin. Moreover, when G90D is expressed in these animals ($G_{0.5}^{+/-}/R^{-/-}$), only a hint of a photosensitive pigment could be detected (Fig. 10F); i.e., if any is present, it is below the sensitivity of the measurements (~0.015 density units).

ERG. To examine the ability of G90D to initiate the phototransduction cascade, we recorded ERGs from 1-month-old WT, $R^{-/-}$, and $G_{0.5}^{+/+}/R^{-/-}$ mice. Figure 11A illustrates a series of responses obtained to stimulus flashes presented to the dark-adapted eye. In comparison to the case for WT mice, higher stimulus intensities were required to elicit a clear response from $R^{-/-}$ or $G_{0.5}/R^{-/-}$ mice, and in both cases the response amplitude increased with increasing flash intensity. Note, however, that, for the $R^{-/-}$ mutant, the highest flash intensities, which evoked a distinct a-wave in WT mice, elicited only a small oscillatory b-wave, with little evidence of a significant

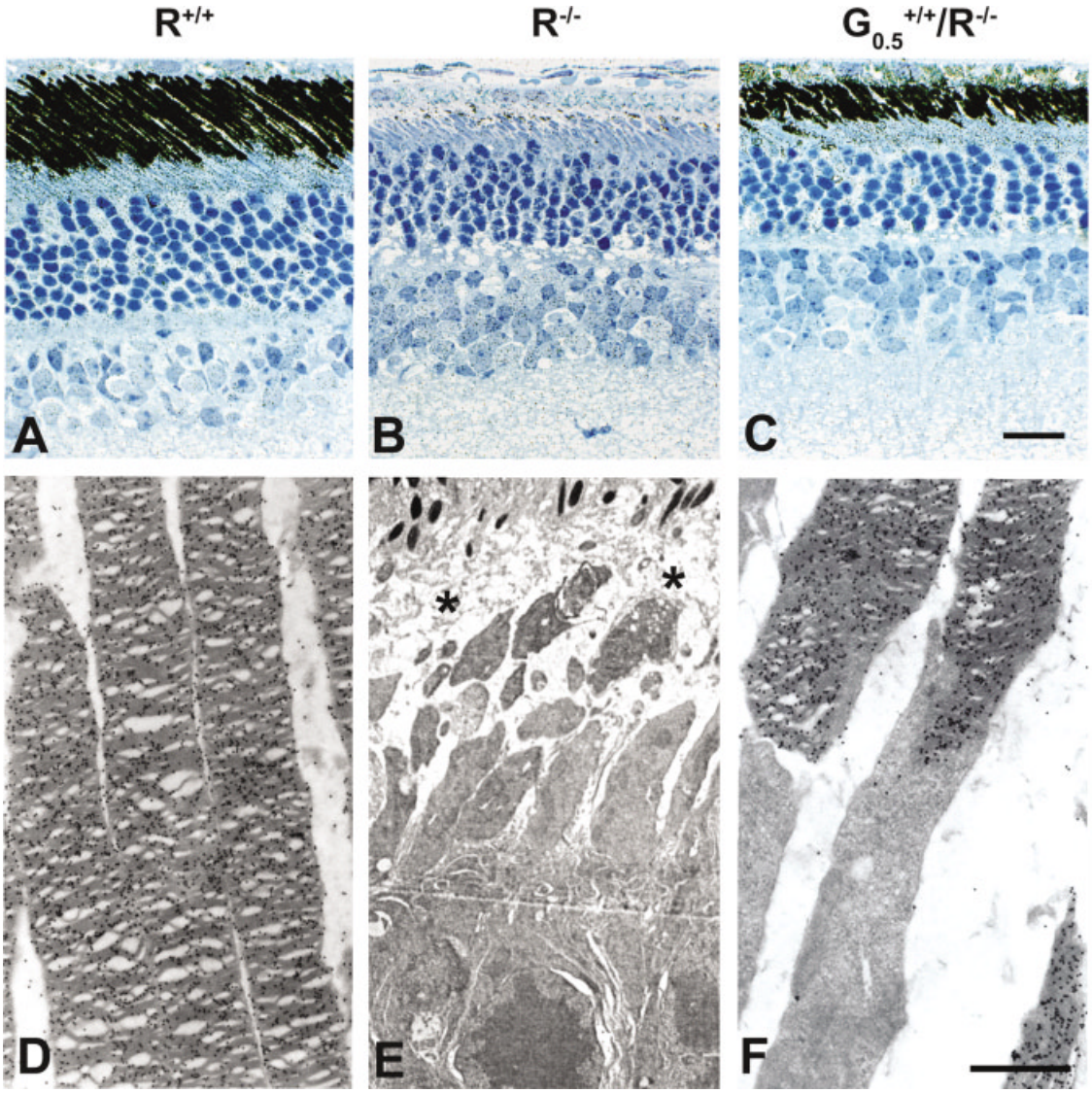

Fig. 8. Immunolocalization of WT and G90D opsin in LM (**A–C**) and EM (**D–F**) images from $R^{+/+}$, $R^{-/-}$, and $G_{0.5}{}^{+/+}/R^{-/-}$ retinas. Note the extensive ROS labeling with rabbit anti-bovine opsin antibody that recognizes both WT and mutant opsins, and the distribution of immunogold particles throughout the disc membranes of WT mice (A,D). No labeling is seen either in the inner nuclear layer or in the cellular debris at the photoreceptor/RPE interface of $R^{-/-}$ mice (B,E). Antibody labeling of the outer segments of $G90D^{+/+}/R^{-/-}$ mice (C,F) shows the proper localization of G90D opsin and its integration into the disc membranes of the ROS. Scale bars = 28 μm in C (applies to A–C); 1 μm in F (applies to D–F).

a-wave. Several lines of evidence indicate that ERGs recorded from $R^{-/-}$ mice reflect exclusively cone-driven activity (Humphries et al., 1997; Lyubarsky et al., 1999; Calvert et al., 2000; Jaissle et al., 2001). In contrast, a distinct a-wave can be seen in the responses recorded from $G_{0.5}/R^{-/-}$ mice, indicating that G90D opsin is able to bind to 11-*cis* retinal and activate rod phototransduction. However, higher flash intensities were required to elicit a response and the a-wave component of the light-evoked responses from $G_{0.5}/R^{-/-}$ mice were much reduced in amplitude compared with those from WT mice. To quantify this reduction, the amplitude of the a-wave was measured at 8 msec after flash onset, a time point that precedes intrusion by the b-wave, and plotted as a function of flash intensity (Fig. 11B). The a-wave response functions for WT and $G_{0.5}/R^{-/-}$ mice both increase with flash intensity up to an asymptotic level. In comparison with the WT responses, the maximal a-wave amplitude of $G_{0.5}/R^{-/-}$ mice is reduced by ~80%, and there is a more than tenfold loss in sensitivity; i.e., the a-wave intensity-response function is shifted to the right by ~1.3 log units.

DISCUSSION

The increasing number of identifiable gene defects associated with human retinal diseases and the development of transgenic technology have led to the creation of numerous mouse models carrying mutations considered

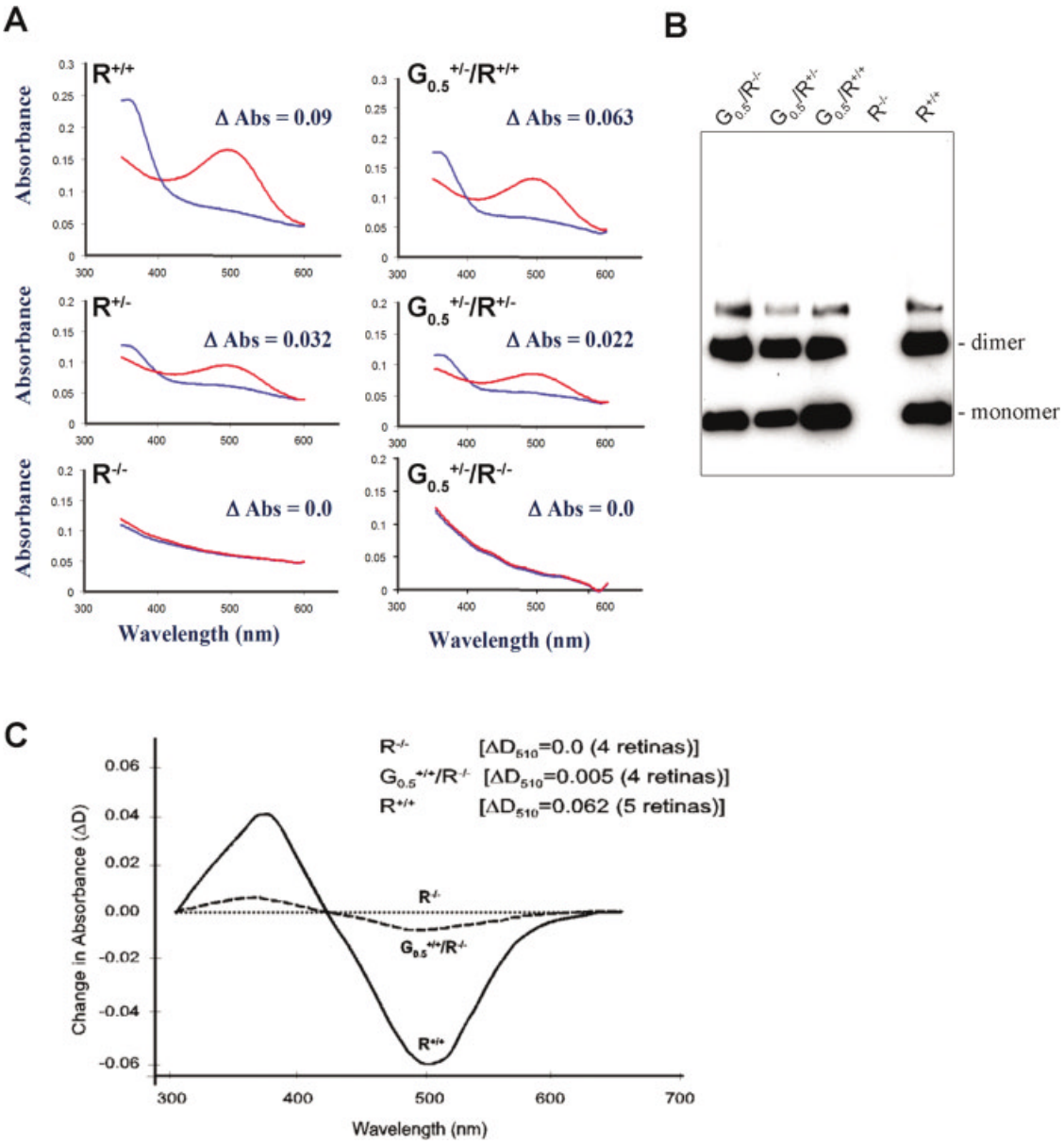

Fig. 9. **A:** Absorbance spectra of ROS membranes isolated from nontransgenic and $G_{0.5}^{+/-}$ retinas in the $R^{+/+}$, $R^{+/-}$, and $R^{-/-}$ backgrounds from dark-adapted preparations (red line) and after bleaching (blue line). A total of 30 μg of ROS protein was used for each spectrum. Note the absence of a 500-nm rhodopsin absorbance peak in recordings on samples from the $R^{-/-}$ and $G_{0.5}^{+/-}/R^{-/-}$ preparations. See text for further details. **B:** Western blot analysis of ROS samples isolated from transgenic and nontransgenic animals in different backgrounds. A total of 20 μg ROS protein was loaded in each lane, and the blot was immunoreacted with mAb 1D4 at a dilution of 1:1,000. No immunoreactivity is seen in the $R^{-/-}$ sample, whereas there is a significant amount of opsin labeling in the G90D/$R^{-/-}$ sample. **C:** Bleaching difference spectra derived from spectrophotometric measurements on retinal extracts from WT (solid line), $G_{0.5}^{+/+}/R^{-/-}$ (dashed line), and $R^{-/-}$ (dotted line) retinas. Recording were obtained before and after completely bleaching the solution, and density losses are plotted as negative values on the ordinates. In the absence of hydroxylamine, a small amount of bleachable pigment (~ 10% of WT) is seen in extracts from the $G_{0.5}^{+/+}/R^{-/-}$ retina. Positive postbleach absorbance values at wavelengths below the isosbestic point represent the formation of the metarhodopsin II photoproduct (λ_{max} ~ 380 nm).

responsible for human conditions. These animals provide a system in which it is possible to examine at various stages of development the pathogenesis of the disease process and the factors that link the genetic anomaly with its phenotype. One drawback to the interpretation of abnormalities presumed to be associated with mutations in the opsin gene is the fact that overexpression of WT opsin can itself induce photoreceptor degeneration (Tan et al., 2001), although this factor may be ameliorated somewhat by the use of the $R^{-/-}$ background.

In addition to transgenic animals, various cell lines transfected with the mutant protein have allowed exhaustive biochemical analysis of the aberrations induced by expression of the mutations causing visual abnormalities.

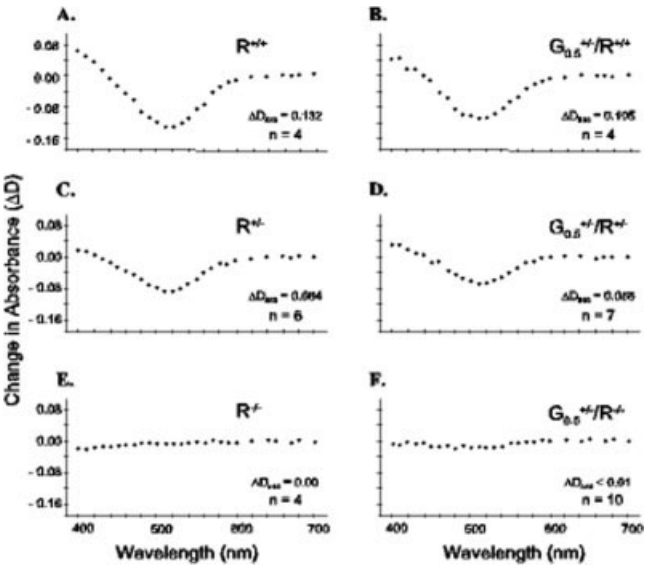

Fig. 10. In situ measurements of absorbance difference spectra $[\Delta D]_\lambda$ recorded from the isolated retinas of 1–2-month-old WT ($R^{+/+}$), heterozygotes ($R^{+/-}$), and rhodopsin knockout ($R^{-/-}$) mice (**A**, **C**, and **E**, respectively) and from $G_{0.5}$ mutants on the three backgrounds (**B**, **D**, and **F**). The data points are averaged from 4 to 10 retinas as indicated and represent the wavelength variation in retinal transmission between spectral scans recorded before and after exposure to an intense bleaching light. Note that density losses after bleaching are plotted as negative values on the ordinates. See text for details.

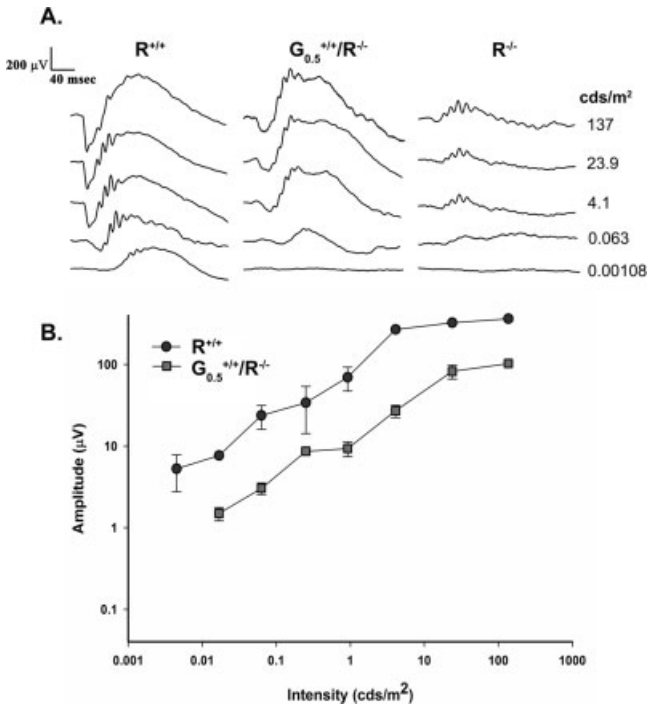

Fig. 11. Dark-adapted electroretinography. **A:** Representative waveforms obtained from 1-month-old $R^{+/+}$ (left), $G_{0.5}{}^{+/+}/R^{-/-}$ (middle), and $R^{-/-}$ (right) mice. Note that $G_{0.5}{}^{+/+}/R^{-/-}$ waveforms include a distinct a-wave that is missing in $R^{-/-}$ responses. **B:** Intensity-response function for the amplitude of the a-wave measured 8 msec after the stimulus flash. Note that the $G_{0.5}{}^{+/+}/R^{-/-}$ function is reduced in amplitude and shifted to the right along the stimulus intensity axis.

The degree to which results obtained from transgenic animals or the cell lines that serve as expression systems reflect the properties of the human disease is always a matter of concern. For some opsin mutations, e.g., P23H, there is good correspondence between the findings obtained in mouse and man (cf. Dryja et al., 1990; Berson et al., 1991; Olsson et al., 1992; Naash et al., 1993; Goto et al., 1995). In others, there appear to be disparities. For example, the K296E opsin mutation, which leads to photoreceptor degeneration in the human retina (Keen et al., 1991; Vaithinathan et al., 1994), was found to produce constitutive activation of transducin when expressed in COS cells (Robinson et al., 1992). However, Li et al. (1995) found no evidence of constitutive activity in ERG recordings from K296E transgenic mice. Although the photoreceptors of these animals undergo progressive degeneration, they showed that the mutant opsin was shut off by inactivation mechanisms that are unlikely to be present in COS cells (i.e., phosphorylation by rhodopsin kinase and arrestin binding) and that render it incapable of activating the photoreceptor transduction cascade.

In the present study, we generated 10 lines of transgenic mice carrying the G90D mutation in the opsin gene (Fig. 1C), a mutation that has been shown to cause a form of CSNB in humans (Sieving et al., 1995), constitutive activation of opsin in COS cells (Rao et al., 1994) and a persistent state of light adaptation ("dark light") in transgenic mice (Sieving et al., 2001). To distinguish between opsin overexpression and the pathology associated with this mutation, three lines were selected for further study based on the expression level of the G90D transgene. Two of the lines ($G_{1.7}$ and $G_{2.5}$) exhibited early signs of photoreceptor degeneration directly related to the levels of opsin overexpression (Fig. 3). The third line ($G_{0.5}{}^{+/-}/R^{+/+}$), expressing one copy of the G90D transgene and opsin levels comparable to normal (Fig. 2B), displayed normal retinal structure up to about 3 months of age (Fig. 4). However, $G_{0.5}{}^{+/-}/R^{+/+}$ mice $\geq$4 months of age showed a progressive loss of photoreceptor nuclei and a progressive shortening of their inner and outer segments (Fig. 4). Because opsin expression in these animals is equivalent to WT, the age-related morphological changes can be attributed to the presence of the mutated opsin. Indeed, it is likely that even low levels of G90D expression would lead ultimately to rod cell death. It is not too surprising, therefore, that patients diagnosed with this form of congenital "stationary" night blindness may show funduscopic signs of retinal abnormalities in later life (Sieving et al., 1995). Moreover, any overexpression of the protein, whether WT or transgenic, will produce a more severe degeneration with earlier onset (Fig. 5).

Although substantial amounts of G90D protein appear to translocate to the ROS of $G_{0.5}{}^{+/-}/R^{-/-}$ photoreceptors, the amount of photosensitive pigment formed is less than 10% of that found in the WT retina (Figs. 9C, 10). Moreover, when the G90D protein is expressed in the visual cells of $R^{+/-}$ and $R^{+/+}$ retinas, the absorbance changes induced by bleaching are less than in the retinas of animals with similar background lacking the G90D transgene (Figs. 9A, 10). A variety of scenarios could account for this phenomenon, but it seems likely that WT opsin ex-

pression is down-regulated or that its bleaching efficacy is reduced by inclusion of the G90D protein. In this regard, our findings are at odds with those obtained from CSNB patients carrying the G90D mutation. In vivo densitometry of these subjects indicates that their retinas contain *normal* amounts of bleachable rhodopsin that regenerates with *faster* than normal kinetics (Sieving et al., 1995). Indeed, the rapid time course of regeneration noted in G90D patients is inconsistent with data obtained from transfected COS cells, in which the rate of association of 11-*cis* retinal with the G90D protein is 80-fold *slower* than with WT opsin (Gross et al., 2003). Clearly, it will be important to address these issues in order to reconcile the differences between data obtained in expression systems (including transgenic animals) and those culled from patients carrying the G90D mutation.

In agreement with Sieving et al. (2001), who also generated transgenic mice expressing G90D opsin, we find that G90D expression in the rhodopsin knockout background serves to induce the development of morphologically intact ROS, enhance the formation of photoreceptor cells, and prolong the survival of the $R^{-/-}$ retina (Fig. 6). However, our observation that the inferior retina of G90D/$R^{-/-}$ mice exhibited greater susceptibility to pathology probably reflects the added insult produced by the greater amount of illumination incident on the inferior retina from the overhead lighting of the housing facility. That disease severity is more pronounced in the inferior retina is seen in other genetically mediated degenerative diseases both in humans (Berson et al., 1991; Kemp et al., 1992) and in transgenic mice (Naash et al., 1996). Nevertheless, photoreceptor survival in mice lacking WT rhodopsin, together with the discrete immunocytochemical localization of opsin to the ROS (Fig. 8), provides convincing evidence that the mutant protein is transported to, and integrated into, the disc membranes of the ROS. Moreover, the photoreceptor potential (a-wave) in the ERG recordings from these animals indicates that some fraction of the G90D opsin present in the ROS is bound to the 11-*cis* retinal chromophore and is capable of activating the phototransduction cascade.

As mentioned above, the phenotype in humans carrying the G90D mutation is characterized by night blindness. Based on findings obtained from expressing this mutation in COS cells, it was concluded that G90D opsin stays in a prolonged state of activation because of the slowed regeneration time, resulting in prolonged activation of transducin signaling (Rao et al., 1994; Gross et al., 2003). However, a consideration of the three-dimensional structure of opsin, and the orientation of the mutated amino acid residues in relation to the chromophore binding site at Lys 296 on opsin, led to the hypothesis that constitutively active mutations operate by a common molecular mechanism, i.e., by disrupting the salt bridge between K296 and the Schiff base counterion, G113 (Dryja et al., 1993; Rao et al., 1994). Interfering with this linkage, which normally constrains opsin in an inactive conformation, could result in deprotonation of the Schiff base, formation of R*, and subsequent activation of the transducin-mediated electrochemical cascade (Cohen et al., 1992). The increased noise of this "dark light,"-like ambient illumination could saturate the rod mechanism and effectively result in night blindness. Studies conducted on members of a large family with autosomal dominant CSNB affected with the G90D mutation (Sieving et al., 1995), as well as the results of an experimental study of G90D mice (Sieving et al., 2001), tend to confirm this interpretation.

Although this mode of action could be responsible for the CSNB phenotype, our results suggest that the ~1.3 log unit loss of sensitivity seen in the ERG of $G_{0.5}{}^{+/+}/R^{-/-}$ mice (Fig. 11B) can be accounted for almost entirely by the loss of quantal absorption associated with the reduced amount of *light-sensitive* pigment in the rod outer segments (Figs. 9C, 10F). In this connection, it is important to recall that, based solely on the loss of quantal absorption, a 90% reduction in the rhodopsin content of the retina would result in a 1 log unit rise in threshold (Ripps, 1982). Comparing the data obtained from the ERG and in situ densitometry on $G_{0.5}{}^{+/+}/R^{-/-}$ mice with the morphological findings is particularly instructive in this regard. The overall amplitude of the a-wave was substantially reduced (to ~20% of WT) in 1-month-old $G_{0.5}/R^{-/-}$ mice, and response sensitivity was reduced by about 1.3 log units (Fig. 11B). In addition, the amount of bleachable photopigment in the retinas of $G_{0.5}/R^{-/-}$ mice was ≤10% of WT. It is unlikely that these abnormalities are manifestations of structural changes resulting from the G90D mutation. No observable reduction in the number of rod photoreceptors or in the lengths of their outer segments were seen in the retinas of $G_{0.5}/R^{-/-}$ mice at P30 to account for such gross changes in either the ERG or the in situ densitometry. Thus, our findings suggest a failure of G90D to complex efficiently with opsin to form a light-sensitive rhodopsin in the ROS. The resultant >90% loss in quantal absorption can readily account for the 1.3 log unit loss in light sensitivity seen in the ERG.

In sum, the ERG a-wave abnormalities and the greatly reduced photosensitive pigment content of $G_{0.5}/R^{-/-}$ mice are consistent with a reduction in quantal absorption resulting from a failure of G90D to complex efficiently with opsin to form a light-sensitive rhodopsin in the ROS. However, additional factors may contribute to the abnormalities seen in these transgenic animals, and we cannot rule out a contribution from a low level of constitutive activity (Sieving et al., 1995) or decreased efficacy of G90D to activate transducin (Zyvaga et al., 1996). Clearly, further biochemical and electrophysiological studies will be required to evaluate the action of the G90D mutation on the in vivo binding and activation of transducin. In addition, more extensive ERG studies are needed to thoroughly define the characteristics of the rod ERG abnormalities of $G_{0.5}$ mice.

ACKNOWLEDGMENTS

We thank Dr. Robert S. Molday (University of British Columbia, Vancouver, British Columbia, Canada) for generously providing the opsin monoclonal antibody (mAb 1D4), Jane Zakevicius for unwavering assistance in various aspects of the research, Barbara Nagel for her excellent technical assistance on the ultrastructural studies, and Drs. Huijun Yang and Ming Cheng for their histology and animal care.

LITERATURE CITED

Al-Jandal N, Farrar GJ, Kiang AS, Humphries MM, Bannon N, Findlay JB, Humphries P, Kenna PF. 1999. A novel mutation within the rhodopsin gene (Thr-94-Ile) causing autosomal dominant congenital stationary night blindness. Hum Mutat 13:75–81.

Alpern M, Holland MG, Oba N. 1972. Rhodopsin bleaching signals in essential night blindness. J Physiol 225:457–476.

Al-Ubaidi MR, Font RL, Quiambao AB, Keener MJ, Liou GI, Overbeek PA, Baehr W. 1990. Bilateral retinal and brain tumors in transgenic mice expressing simian virus 40 large T antigen under control of the human interphotoreceptor retinoid-binding protein promoter. J Cell Biol 119:1681–1687.

Berson EL. 1993. Retinitis pigmentosa. The Friedenwald Lecture. Invest Ophthalmol Vis Sci 34:1659–1676.

Berson EL, Rosner B, Sandberg MA, Dryja TP. 1991. Ocular findings in patients with autosomal dominant retinitis pigmentosa and a rhodopsin gene defect (Pro-23-His). Arch Ophthalmol 109:92–101.

Calvert PD, Krasnoperova NV, Lyubarsky AL, Isayama T, Nicolo M, Kosaras B, Wong G, Gannon KS, Margolskee RF, Sidman RL, Pugh EN Jr, Makino CL, Lem J. 2000. Phototransduction in transgenic mice after targeted deletion of the rod transducin alpha-subunit. Proc Natl Acad Sci U S A 97:13913–13918.

Carr RE, Ripps H, Siegel IM, Weale RA. 1966. Rhodopsin and the electrical activity of the retina in congenital night blindness. Invest Ophthalmol 5:497–507.

Cohen GB, Oprian DD, Robinson PR. 1992. Mechanism of activation and inactivation of opsin: role of Glu113 and Lys296. Biochemistry 31: 12592–125601.

Danciger M, Blaney J, Gao YQ, Zhao DY, Heckenlively JR, Jacobson SG, Farber DB. 1995. Mutations in the PDE6B gene in autosomal recessive retinitis pigmentosa. Genomics 30:1–7.

Dryja TP, McGee TL, Hahn LB, Cowley GS, Olsson JE, Reichel E, Sandberg MA, Berson EL. 1990. Mutations within the rhodopsin gene in patients with autosomal dominant retinitis pigmentosa. N Engl J Med 323:1302–1307.

Dryja TP, Berson EL, Rao VR, Oprian DD. 1993. Heterozygous missense mutation in the rhodopsin gene as a cause of congenital stationary night blindness. Nat Genet 4:280–283.

Dryja TP, Finn JT, Peng, YW, McGee TL, Berson EL, Yau KW. 1995. Mutations in the gene encoding the alpha subunit of the rod cGMP-gated channel in autosomal recessive retinitis pigmentosa. Proc Natl Acad Sci U S A 92:10177–10181.

Erickson PA, Lewis GP, Fisher SK. 1993. Post-embedding immunocytochemical techniques for light and electron microscopy. Methods Cell Biol 37:283–310.

Fung BK. 1983. Characterization of transducin from bovine retinal rod outer segments. I. Separation and reconstitution of the subunits. J Biol Chem 258:10495–10502.

Gal A, Orth U, Baehr W, Schwinger E, Rosenberg T. 1994. Heterozygous missense mutation in the rod cGMP phosphodiesterase beta-subunit gene in autosomal dominant stationary night blindness. Nat Genet 7:64–68.

Garriga P, Manyosa J. 2002. The eye photoreceptor protein rhodopsin. Structural implications for retinal disease. FEBS Lett 528:17–22.

Goto Y, Peachey NS, Ripps H, Naash MI. 1995. Functional abnormalities in transgenic mice expressing a mutant rhodopsin gene. Invest Ophthalmol Vis Sci 36:62–71.

Gross AK, Xie G, Oprian DD. 2003. Slow binding of retinal to rhodopsin mutants G90D and T94D. Biochemistry 42:2002–2008.

Hodges RS, Heaton RJ, Parker JM, Molday L, Molday RS. 1988. Antigen-antibody interaction. Synthetic peptides define linear antigenic determinants recognized by monoclonal antibodies directed to the cytoplasmic carboxyl terminus of rhodopsin. J Biol Chem 263:11768–11775.

Huang SH, Pittler SJ, Huang X, Oliveira L, Berson EL, Dryja TP. 1995. Autosomal recessive retinitis pigmentosa caused by mutations in the alpha subunit of rod cGMP phosphodiesterase. Nat Genet 11:468–471.

Humphries P, Kenna P, Farrar GJ. 1992. On the molecular genetics of retinitis pigmentosa. Science 256:804–808.

Humphries MM, Rancourt D, Farrar GJ, Kenna P, Hazel M, Bush RA, Sieving PA, Sheils DM, McNally N, Creighton P, Erven A, Boros A, Gulya K, Capecchi MR, Humphries P. 1997. Retinopathy induced in mice by targeted disruption of the rhodopsin gene. Nat Genet 15:216–219.

Jaissle GB, May CA, Reinhard J, Kohler K, Fauser S, Lutjen-Drecoll E, Zrenner E, Seeliger MW. 2001. Evaluation of the rhodopsin knockout mouse as a model of pure cone function. Invest Ophthalmol Vis Sci 42:506–513.

Keen TJ, Inglehearn CF, Lester DH, Bashir R, Jay M, Bird AC, Jay B, Bhattacharya SS. 1991. Autosomal dominant retinitis pigmentosa: four new mutations in rhodopsin, one of them in the retinal attachment site. Genomics 11:199–205.

Kemp CM, Jacobson SG, Roman AJ, Sung CH, Nathans J. 1992. Abnormal rod dark adaptation in autosomal dominant retinitis pigmentosa with proline-23-histidine rhodopsin mutation. Am J Ophthalmol 113:165–174.

Lem J, Krasnoperova NV, Calvert PD, Kosaras B, Cameron DA, Nicolo M, Makino CL, Sidman RL. 1999. Morphological, physiological, and biochemical changes in rhodopsin knockout mice. Proc Natl Acad Sci U S A 96:736–741.

Li T, Franson WK, Gordon JW, Berson EL, Dryja TP. 1995. Constitutive activation of phototransduction by K296E opsin is not a cause of photoreceptor degeneration. Proc Natl Acad Sci U S A 92:3551–3555.

Lowry OH, Rosebrough NJ, Lewis Farr J, Randall RJ. 1951. Protein measurement with the Folin phenol reagent. J Biol Chem 193:265–275.

McLaughlin ME, Sandberg MA, Berson EL, Dryja TP. 1993. Recessive mutations in the gene encoding the beta-subunit of rod phosphodiesterase in patients with retinitis pigmentosa. Nat Genet 4:130–134.

Naash MI, Hollyfield JG, al-Ubaidi MR, Baehr W. 1993. Simulation of human autosomal dominant retinitis pigmentosa in transgenic mice expressing a mutated murine opsin gene. Proc Natl Acad Sci U S A 90:5499–5503.

Naash MI, Ripps H, Li S, Goto Y, Peachey NS. 1996. Polygenic disease and retinitis pigmentosa: albinism exacerbates photoreceptor degeneration induced by the expression of a mutant opsin in transgenic mice. J Neurosci 16:7853–7858.

Olsson JE, Gordon JW, Pawlyk BS, Roof D, Hayes A, Molday RS, Mukai S, Cowley GS, Berson EL, Dryja TP. 1992. Transgenic mice with a rhodopsin mutation (Pro23His): a mouse model of autosomal dominant retinitis pigmentosa. Neuron 9:815–830.

Palmiter RD, Brinster RL. 1986. Germ-line transformation of mice. Annu Rev Genet 20:465–499.

Peachey NS, Fishman GA, Kilbride PE, Alexander KR, Keehan KM, Derlacki DJ. 1990. A form of congenital stationary night blindness with apparent defect of rod phototransduction. Invest Ophthalmol Vis Sci 31:237–246.

Pittler SJ. Baehr W. 1991. Identification of a nonsense mutation in the rod photoreceptor cGMP phosphodiesterase beta-subunit gene of the rd mouse. Proc Natl Acad Sci U S A 88:8322–8326.

Rao VR, Cohen GB, Oprian DD. 1994. Rhodopsin mutation Gly90Asp and a molecular mechanism for congenital night blindness. Nature 367:639–642.

Ripps H. 1982. Night blindness revisited: from man to molecules. Invest Ophthalmol 23:588–609.

Ripps H, Snapper AG. 1974. Computer analysis of photochemical changes in the human retina. Comput Biol Med 4:107–122.

Robinson PR, Cohen GB, Zhukovsky EA, Oprian DD. 1992. Constitutively active mutants of rhodopsin. Neuron 9:719–725.

Robinson PR, Buczylko J, Ohguro H, Palczewski K. 1994. Opsins with mutations at the site of chromophore attachment constitutively activate transducin but are not phosphorylated by rhodopsin kinase. Proc Natl Acad Sci U S A 91:5411–5415.

Schoenlein RW, Peteanu LA, Mathies RA, Shank CV. 1991. The first step in vision: femtosecond isomerization of rhodopsin. Science 254:412–415.

Sieving PA, Richards JE, Naarendorp F, Bingham EL, Scott K, Alpern M. 1995. Dark-light: model for nightblindness from the human rhodopsin Gly-90→Asp mutation. Proc Natl Acad Sci U S A 92:880–884.

Sieving PA, Fowler ML, Bush RA, Machida S, Calvert PD, Green DG, Makino CL, McHenry CL. 2001. Constitutive "light" adaptation in rods from G90D rhodopsin: a mechanism for human congenital nightblindness without rod cell loss. J Neurosci 21:5449–5460.

Stojanovic A, Hwa J. 2002. Rhodopsin and retinitis pigmentosa: shedding light on structure and function. Recept Channels 8:33–50.

Tan E, Wang Q, Quiambao AB, Xu X, Qtaishat NM, Peachey NS, Lem J, Fliesler SJ, Pepperberg DR, Naash MI, Al-Ubaidi MR. 2001. The relationship between opsin overexpression and photoreceptor degeneration. Invest Ophthalmol Vis Sci 42:589–600.

Travis GH. 1998. Mechanisms of cell death in the inherited retinal degenerations. Am J Hum Genet 62:503–508.

Vaithinathan R, Berson EL, Dryja TP. 1994. Further screening of the rhodopsin gene in patients with autosomal dominant retinitis pigmentosa. Genomics 21:461–463.

Weale RA. 1953. Photochemical reactions in the living cat's retina. J Physiol 122:322–331.

Williams TP, Henrich S, Reiser M. 1998. Effect of eye closures and openings on photostasis in albino rats. Invest Ophthalmol Vis Sci. 39:603–609.

Wu TH, Ting TD, Okajima TI, Pepperberg DR, Ho YK, Ripps H, Naash MI. 1998. Opsin localization and rhodopsin photochemistry in a transgenic mouse model of retinitis pigmentosa. Neuroscience 87:709–717.

Zuyaga TA, Fahmy K, Siebert F, Sakmar TP. 1996. Characterization of mutant visual pigment responsible for congenital night blindness: a biochemical and Fourier-transform infrared spectroscopy study. Biochemistry 35:7536–7545.